

**On the Numerical Calculation of
Electromagnetic Fields Generated by
Ocean Currents**

**Robert H. Tyler and Lawrence A. Mysak
C²GCR Report No. 95-5
April 1995**

On the Numerical Calculation of Electromagnetic Fields Generated by Ocean Currents

Robert H. Tyler and Lawrence A. Mysak

April 1995

Department of Atmospheric and Oceanic Sciences
and

Centre for Climate and Global Change Research

McGill University

805 Sherbrooke St. W.

Montréal, Québec, H3A 2K6

Phone: R. Tyler (514 398-4770); L.A. Mysak (514 398-3759)

Fax: 514 398-1381

email: rob@iemanja.meteo.mcgill.ca

Abstract

In this paper we compare two approaches (model formulations) for finding simple explicit numerical solutions for the electromagnetic fields generated by three-dimensional ocean currents. The first approach, based on the induction equation, is the relevant one when dealing with realistic time-dependent ocean current and conductivity fields. In many cases, this approach will, however, be computationally unfeasible due to the small time steps required for numerical stability. The second approach is based on the electropotential equation and requires quasistasis. The numerical solutions using this approach converge quite quickly, suggesting that this method could be viably employed to calculate the fields due to high-resolution three-dimensional (quasisteady) ocean circulation.

1 Introduction

In the ocean, salts such as NaCl exist largely as dissociated ions. As ocean currents advect these ions through the earth's magnetic field, Lorentz forces on the ions lead to the generation of electrical fields, electrical currents, and secondary magnetic fields. Electrical forces tending to change the ocean flow exist but are negligibly small.

In recent years it has been realized that ocean circulation and its variability play a crucial role in determining the earth's climate and its fluctuations. Since the ocean currents induce magnetic fields, it has been pointed out that a wealth of ocean current (and hence climate) proxy data may be distilled from the existing geomagnetic record (Stephenson and Bryan, 1992; Tyler, 1992; Winch and Runcorn, 1993; Tyler and Mysak, 1993, 1994, 1995b). There is thus a strong motivation for better understanding the electromagnetic fields generated by ocean currents.

Although a reasonable amount of theoretical work has been done on this subject (Longuet-Higgins *et al.*, 1954; Sanford, 1971; Chave, 1983; Chave and Luther, 1990; Tyler and Mysak, 1993, 1994, 1995b), analytical solutions can only be found for idealized conductivity and current velocity fields. Thus numerical techniques are necessary to treat more realistic cases (Sanford *et al.*, 1990).

An important numerical study has been published by Stephenson and Bryan (1992). They found solutions for the 2-D electromagnetic field induced by the annual mean and first annual harmonic of the global ocean circulation at two-degree resolution. In their approach, they solved a 2-D equation that is based on the time-independent induction equation using an under-relaxation technique. They used depth-integrated forms of the conductivity and ocean current velocities, and further, they employed only two conductivity values (land, ocean). These idealizations were made despite the facts that baroclinic currents are often more efficient than barotropic currents as generators of magnetic fields, and that variations in

conductivity in the oceans and ocean sediments are significant. Still, there are at least two reasons for their approach. First, even though the magnetic fields induced by baroclinic currents as measured within the water are dominant, the vertical component of the induced magnetic field measured above the sea-surface may be largely dependent on only depth-integrated forms of the velocity and conductivity. Second, and perhaps most significant, the explicit numerical scheme they used does not appear to converge quickly. A more realistic global 3-D model using a similar numerical scheme does not currently seem feasible. Stephenson and Bryan have suggested that other algorithms should be investigated.

Before entering into more complicated implicit methods, it is natural to investigate whether other formulations using explicit methods can be used feasibly.

The main purpose of this paper is to show that an explicit numerical approach based on the electropotential equation (rather than the induction equation) can be used easily and efficiently in calculating the steady-state ocean-induced electromagnetic fields. We start, however, by presenting a numerical model based on the time-dependent induction equation in §2. We run this model with steady forcing and obtain results for a test case that are compared in §4 with results obtained from the electropotential equation-based model presented in §3.

The induction equation can be solved numerically to give a complete description of the time evolution of the electromagnetic field due to general time-dependent ocean conductivity and flow. The basic problem—with explicit numerical schemes, at least—is that very small time steps are required for numerical stability, which make even integrating to a steady-state quite expensive. The steady-state electropotential equations may, in contrast, be solved much less expensively. From the steady-state electropotential equation and the use of additional assumptions, the steady-state magnetic field may be obtained. We return to a more specific comparison between these two approaches in the final section.

2 Approach Based on the Induction Equation

In Tyler and Mysak (1995a), we used principles from General Relativity theory to derive the set of equations that apply for observers in a rotating (accelerating) reference frame studying the electrodynamics of a material medium moving with velocity relative to the rotating frame. For the particular application where the material medium is the ocean moving with relative velocity \mathbf{u}_c in the rotating frame of the solid earth, and considering typical parameter values for the electric properties of the terrestrial system, we found that to a very good approximation the following equations of electromagnetism can be used:

$$\nabla \times \mathbf{E} = \partial_t \mathbf{B}, \quad (1)$$

$$\nabla \cdot \mathbf{B} = 0, \quad (2)$$

$$\nabla \times \mathbf{B} = \mu_o \mathbf{J}, \quad (3)$$

$$\nabla \cdot (\epsilon \mathbf{E} - \frac{\epsilon}{N^2} \tilde{\mathbf{u}} \times \mathbf{B}) = \rho_e, \quad (4)$$

$$\mathbf{J} = \sigma (\mathbf{E} + \mathbf{u}_c \times \mathbf{B}), \quad (5)$$

where \mathbf{u}_c is the ocean current velocity relative to the solid earth (with solid-body rotation velocity \mathbf{u}_s), and $\tilde{\mathbf{u}} = \mathbf{u}_s + \mathbf{u}_c(1 - N^2)$ in which the index of refraction N is defined as $N = (\mu_r \epsilon_r)^{1/2}$. The other symbols are standard and represent the electric field strength (\mathbf{E}), magnetic flux density (\mathbf{B}), electric current density (\mathbf{J}), electric volume charge density (ρ_e), the electric conductivity ($\sigma \approx 3 - 5$ S/m for seawater), electric permittivity ($\epsilon = \epsilon_r \epsilon_o$, where ϵ_r is the relative permittivity of the material (≈ 80 for seawater), and $\epsilon_o = 8.854 \times 10^{-12}$ F/m is the permittivity of free space), and the magnetic permeability ($\mu = \mu_r \mu_o$, where μ_r is the relative magnetic permeability (taken to be = 1 in this study) and $\mu_o = 4\pi \times 10^{-7}$ H/m is the magnetic permeability of free space).

The fact that (1)–(3) and (5) retain a form similar to their inertial-frame forms depends both on the small rotational accelerations as well as the electric properties of the terrestrial media (see Tyler and Mysak (1995a) for more details).

Using (1)–(3) and (5), we can construct a form of the induction equation that is also similar to the inertial-frame form (Tyler and Mysak, 1995a):

$$\partial_t \mathbf{B} = \nabla \times (\mathbf{u}_c \times \mathbf{B}) - \nabla K \times (\nabla \times \mathbf{B}) + K \nabla^2 \mathbf{B} \quad (6)$$

where $K = (\mu_o \sigma)^{-1}$ is the magnetic diffusion coefficient. Given an ocean-current field, \mathbf{u}_c (from now on we will leave off the subscript) and conductivity field, (6) is used to solve for the magnetic field \mathbf{B} .

Due to (2), ocean-induced magnetic fields will decay to zero away from the oceanic sources. To satisfy this condition approximately in the numerical model, we let $\mathbf{B} = \mathbf{F} + \mathbf{b}$ where \mathbf{F} is the specified earth’s main magnetic field and \mathbf{b} is the ocean-induced component, and we impose Neuman boundary conditions on \mathbf{b} on the faces of the 3-D finite-difference Cartesian grid domain. The domain is chosen such that the Lorentz forces $\mathbf{u} \times \mathbf{B}$ are small near the boundaries.

Here we will use a simple explicit numerical solution method. All variables are defined at every grid point. We represent the time derivative using FIT (forward in time) differencing. We use a seven grid-point representation for the Laplacian terms and a CIS (centered in space) discretization scheme for first-order spatial derivatives (for numerical stability, we use upstream differencing for $\partial_z \mathbf{B}$ at the air/water conductivity interfaces). For numerical stability, the time step is chosen to satisfy

$$\Delta t < \text{minimum} \left\{ \frac{((\Delta x)^{-2} + (\Delta y)^{-2} + (\Delta z)^{-2})^{-1/2}}{|\mathbf{u}|}, \frac{((\Delta x)^{-2} + (\Delta y)^{-2} + (\Delta z)^{-2})^{-1}}{4K} \right\} \quad (7)$$

where $\Delta x, \Delta y, \Delta z$ are the grid-point spacings.

Given an initial condition $\mathbf{b}(x, y, z, t = 0)$ and specified $K, \mathbf{u}, \mathbf{F}$, forward time-stepping can be used to obtain the magnetic field $\mathbf{B} = \mathbf{F} + \mathbf{b}$ at later times. From \mathbf{B} and equations (3) and (5), we can also obtain \mathbf{J} and \mathbf{E} .

For simple illustration, and for comparison with the results to be presented in the next section, we apply the model to the following specific case of a small-scale

gyre under a uniform vertically-directed main field $\mathbf{F} = F_z \hat{z}$ (which will be fast to compute): We use uniform horizontal and non-uniform vertical grid spacing which is defined by the stretched vertical coordinate $z(k)$ as

$$z = \beta^{-1} \Delta z|_{z=0} \sinh[\beta(k - k_o)]. \quad (8)$$

The grid spacing (obtained through differentiation of (8) with respect to k) is

$$\Delta z = \Delta z|_{z=0} \cosh[\beta(k - k_o)], \quad (9)$$

where $\Delta z|_{z=0}$ is the thickness of the layer at the sea surface, β is a stretching parameter, and k_o is the level index corresponding with the sea surface. For this case, we choose $\Delta z|_{z=0} = 100$ m, $\beta = 8/k_{max}$, and $k_o = 12$. Also, we use a grid domain of 15×15 points in the horizontal with 20 vertical levels ($k_{max} = 20$). We choose the horizontal grid spacing $\Delta x = \Delta y = 10^3$ m. Figure 1 shows the mapping between the physical vertical coordinate and vertical grid-point indices. The 3-D array with indices i, j, k (Figure 2a) samples the 3-D physical domain having coordinates x, y, z (Figure 2b). We will present all our results in the index space shown in Figure 2a since this will better show the area of interest. The frequency of sampling is highest near $z = 0$ where the greatest velocity shear and conductivity changes occur. The model accepts an arbitrary conductivity field. For the present sample demonstration, we will consider K to have only 3 values: within the ocean ($-5 \times 10^3 \text{ m} \leq z \leq 0$), $K = K_o = 2 \times 10^5 \text{ m}^2/\text{s}$; in the air ($z > 0$), $K = 10^2 \times K_o$; in the sediments ($z < -5 \times 10^3 \text{ m}$), $K = 10 \times K_o$.

We consider a velocity field that is everywhere zero except within a layer $-100 \text{ m} \leq z \leq 0$ where the x and y components have the form

$$u = \frac{f_1}{\max(f_1)} \quad (10)$$

and

$$v = \frac{f_2}{\max(f_2)} \quad (11)$$

with

$$f_1 = -\cos\left(\frac{\pi y}{y_{max}}\right)\sin\left(\frac{\pi y}{x_{max}}\right)re^{-1/18(r/x_{max})^2}, \quad (12)$$

$$f_2 = \cos\left(\frac{\pi x}{x_{max}}\right)\sin\left(\frac{\pi y}{y_{max}}\right)re^{-1/18(r/x_{max})^2}, \quad (13)$$

and $r = \sqrt{(x - .5x_{max})^2 + (y - .5y_{max})^2}$. In the case considered here, $x_{max} = y_{max} = 15$. The velocity components u, v have been normalized such that the maximum values are equal to 1 m/s. The gyre velocities are depicted in Figures 3a,b. We take the initial condition $\mathbf{b}(t = 0) = 0$.

In Figure 4 we show the normalized x -component of the induced horizontal magnetic field (b_x/F_z). To indicate the approach to steady-state, the mean root-squared values of b_x/F_z as a function of time are shown in Figure 5.

The numerical model we used was written in *Matlab* and was run on an IBM RISC 6000 workstation. The model took 1.7 s of cpu per time step. The value for Δt in this case was $\Delta t = 4.8 \times 10^{-4}$ s. In obtaining the solution shown in Figure 4, a total of 21359 iterations (3.6×10^4 seconds of cpu) were used.

3 Approach Based on the Electropotential Equation

Under steady state conditions, equation (1) gives $\nabla \times \mathbf{E} = 0$. Hence, we can write $\mathbf{E} = \nabla\psi$, where ψ is a scalar electropotential function. Then, taking the divergence of (5), noting that $\nabla \cdot \mathbf{J} = 0$ by (2) and assuming $|\nabla \cdot (\sigma \mathbf{u} \times \mathbf{b})| \ll |\nabla \cdot (\sigma \mathbf{u} \times \mathbf{F})|$ (the results must be checked afterwards to validate this assumption), we have after some rearrangement of the terms,

$$\nabla \cdot (\sigma \nabla \psi) = -\nabla \cdot (\sigma \mathbf{u} \times \mathbf{F}) \quad (14)$$

which for specified $\sigma, \mathbf{u}, \mathbf{F}$ involves only the unknown ψ .

There are many numerical methods for solving (14). Here, we use sequential relaxation due to its simplicity and generality. We first write (14) as

$$\nabla^2 \psi = -\frac{1}{\sigma} \nabla \cdot (\sigma \mathbf{u} \times \mathbf{F}) - \nabla \ln \sigma \cdot \nabla \psi. \quad (15)$$

As in the last section, we use a seven grid-point representation for the Laplacian term and a CIS discretization scheme for the first order derivatives. An iterative scheme for solving (15) is then

$$\psi_{i,j,k}^{n+1} = \psi_{i,j,k}^n + \frac{\alpha}{2((\Delta x)^{-2} + (\Delta y)^{-2} + (\Delta z)^{-2})} R \quad (16)$$

where R is the residual

$$R = \nabla^2 \psi + \frac{1}{\sigma} \nabla \cdot (\sigma \mathbf{u} \times \mathbf{F}) + \nabla \ln \sigma \cdot \nabla \psi, \quad (17)$$

i, j, k refer to the 3-D grid-point indices, n is the iteration number and α is the relaxation coefficient satisfying $0 < \alpha < 2$. We use a grid domain in which the boundaries are far enough away from the forcing centers such that the outward-directed electric field vector magnitude is small on the boundary, allowing us to impose Neuman boundary conditions on ψ at the boundaries.

Once ψ is found, \mathbf{E} is obtained from $\mathbf{E} = \nabla \psi$. Then, \mathbf{J} can be found using Ohm's law (5), with the approximation $\mathbf{u} \times \mathbf{B} \approx \mathbf{u} \times \mathbf{F}$ (as stated earlier, the subscript on the velocity appearing in (5) has been dropped). With \mathbf{J} known, we can solve for \mathbf{b} in the following way: First note that by assumption, \mathbf{F} involves only electrical currents in the earth's core; hence, outside of the core, (3) requires

$$\nabla \times \mathbf{B} = \nabla \times (\mathbf{F} + \mathbf{b}) = \nabla \times \mathbf{b} = \mu_o \mathbf{J}. \quad (18)$$

We next take the curl of (18). After using appropriate vector identities (and invoking $\nabla \cdot \mathbf{b} = 0$), we obtain the vector Poisson equation

$$\nabla^2 \mathbf{b} = -\mu_o \nabla \times \mathbf{J}. \quad (19)$$

In the Cartesian domain, (19) is easily separated into three scalar Poisson equations:

$$\nabla^2 b_x = -\mu_o (\nabla \times \mathbf{J}) \cdot \hat{x}, \quad (20)$$

$$\nabla^2 b_y = -\mu_o (\nabla \times \mathbf{J}) \cdot \hat{y}, \quad (21)$$

$$\nabla^2 b_z = -\mu_o (\nabla \times \mathbf{J}) \cdot \hat{z}, \quad (22)$$

which we solve using boundary conditions and relaxation techniques identical to that used in solving for ψ . We find solutions for forcing due to the ocean gyre described in the last section. Cross-sections of the solutions for ψ and b_x are shown in Figures 6a,b. The convergence of the residuals are shown in Figures 7a,b. The approximation $|\nabla \cdot (\sigma \mathbf{u} \times \mathbf{b})| \ll |\nabla \cdot (\sigma \mathbf{u} \times \mathbf{F})|$ was justified in this case since the values of $|\nabla \cdot (\sigma \mathbf{u} \times \mathbf{b})|$ were found to be at least two orders of magnitude smaller than the values of $|\nabla \cdot (\sigma \mathbf{u} \times \mathbf{F})|$.

We see by comparing figures 4 and 6 that the b_x calculated using the electropotential equation is in fact similar to that calculated using the induction equation, with b_x from the induction equation having a magnitude slightly smaller due to the fact that it has not completely reached steady state.

The numerical model we used was written in *Matlab* and was run on an IBM RISC 6000 workstation. The solver for ψ took 0.26 s of cpu per iteration. The solver for the \mathbf{b} terms took slightly less time (0.24 s per iteration) due to a few less terms in the equation that needed to be calculated. To obtain the solution in Figure 6a, 30,000 iterations were used, and to obtain the solution shown in Figure 6b, 1007 iterations were used. The total cpu time used was 8.0×10^3 seconds. This can be compared with the induction equation solution which, as stated in the last section, used 3.6×10^4 seconds of cpu. Other experiments we have conducted indicate that the efficiency of the potential-based approach over the induction-based approach is even greater when we use larger-scale ocean forcing features with a smaller aspect ratio (ratio of depth scale to length scale).

4 Discussion

In this paper we have investigated two simple explicit methods for numerically calculating the electromagnetic fields generated by ocean currents. The results we have found indicate that a model based on the electropotential equation appears to be computationally much less expensive than a model based on the induction equation. The electropotential equation, however, is only applicable to

a quasisteady balance between the electromagnetic fields and the ocean current and conductivity fluctuations. Solving the steady-state induction equation using an explicit relaxation scheme as done for ψ is also expected to converge slowly since, as described in Stephenson and Bryan (1992), the explicit time-stepping and relaxation methods are quite similar for the problem considered here with a step-function forcing. That is, the small Δt required (due to the combination of the large diffusion coefficient K and small Δz) in the time-stepping approach would translate in the relaxation scheme as a great number of iterations required to attain convergence.

These results should be regarded with caution, however, since comparison between the two approaches is not straightforward. For example, if the main interest is in the magnetic field (which in the electropotential-based model involves calculations using gradients in the electropotential field), the convergence criteria may need to be more strict than the criteria used in the induction equation-based model (which calculates the magnetic field directly). The importance of these considerations will depend on the particular application.

A few clear advantages of the electropotential approach can be pointed out: The induction-equation approach requires time-stepping three equations (one for each of the three magnetic field components) simultaneously. The electropotential approach requires the solution of four equations (for the electropotential ψ and the three magnetic vector components). However, unlike the induction-equation approach, the electropotential approach gives uncoupled Poisson equations for the three magnetic components. Hence, not all three need to be solved for, or, the three could be solved for in parallel once ψ has been found. Hence, if the main interest is in calculating only the vertical component of the magnetic field, for instance, the electropotential approach involves solving two uncoupled Poisson equations while the induction-equation approach involves time-stepping three coupled equations.

Furthermore, if our interest is only to have solutions for \mathbf{b} above the sea surface

(where observations are made), the most efficient strategy might be to solve for ψ and then b_z only. Treating the region above the sea surface as an insulator, the magnetic field is derivable from a scalar potential ($\nabla \times \mathbf{b} = \mathbf{J} = 0$, hence $\mathbf{b} = \nabla\phi$ where ϕ is a scalar potential). Then, since $\nabla \cdot \mathbf{b} = 0$, $\nabla^2\phi = 0$, which can be solved in the regions $0 \leq z$ given the boundary conditions $\partial_z\phi(z=0) = b_z(z=0)$ and $\partial_z\phi(z \rightarrow \infty) = 0$. Using this method we would obtain $\mathbf{b}(0 \leq z)$ after sequentially solving three scalar Poisson equations—one of which would be solved in the smaller domain $0 \leq z$. This should invariably have advantages over the induction-equation approach which requires the simultaneous solution of three coupled equations over the entire domain.

Acknowledgements

LAM is grateful to the Canadian Natural Sciences and Engineering Research Council for research support for this work.

References

- CHAVE, A. D. (1983). On the theory of electromagnetic induction in the earth by ocean currents. *Journal of Geophysical Research*, 88:3531–3542.
- CHAVE, A. D. AND LUTHER, D. S. (1990). Low-frequency, motionally-induced electromagnetic fields in the ocean. *Journal of Geophysical Research*, 95:7185–7200.
- LONGUET-HIGGINS, M. S., STERN, M. E., AND STOMMEL, H. (1954). The electrical field induced by ocean currents and waves, with applications to the method of towed electrodes. Papers in physical oceanography and meteorology 1, WHOI and MIT, Cambridge and Woods Hole. 37 pp.
- SANFORD, T. B. (1971). Motionally induced electric fields in the sea. *Journal of Geophysical Research*, 76:3476–3493.
- SANFORD, T. B., CHAVE, A. D., LUTHER, D. S., COX, C. S., FILLOUX, J. H., AND LARSEN, J. C. (1990). Motional electromagnetic methods and WOCE. Report 3, U.S. WOCE Office, College Station, TX. 42 pp.
- STEPHENSON, D. AND BRYAN, K. (1992). Large-scale electric and magnetic fields generated by the oceans. *Journal of Geophysical Research*, 97:15467–15480.
- TYLER, R. H. (1992). The potential for using geomagnetic data as proxy for river discharge into the arctic and a review of other potential proxies. Report 92-16, Centre for Climate and Global Change Research, McGill University.
- TYLER, R. H. AND MYSAK, L. A. (1993). The potential for using geomagnetic data in ocean and climate studies. I: Theory of electromagnetic fields induced by ocean currents. Report 93-20, Centre for Climate and Global Change Research, McGill University.

- TYLER, R. H. AND MYSAK, L. A. (1994). The potential for using geomagnetic data in ocean and climate studies. III: Electromagnetic fields generated by idealized ocean circulation. Report 94-9, Centre for Climate and Global Change Research, McGill University.
- TYLER, R. H. AND MYSAK, L. A. (1995a). Electrodynamics in a rotating frame of reference with application to global ocean circulation. *Canadian Journal of Physics*, accepted January, 1995.
- TYLER, R. H. AND MYSAK, L. A. (1995b). Motionally-induced electromagnetic fields generated by idealized ocean circulation. accepted by *Geophysical and Astrophysical Fluid Dynamics*.
- WINCH, D. E. AND RUNCORN, S. K. (1993). Geomagnetic observatory data and ocean circulation. *Exploration Geophysics*, 24:139-144.

Figure 1:

Mapping of physical vertical coordinate and vertical array index.

Figure 2:

Model domain in index space (a) and physical space (b).

Figure 3:

Ocean gyre velocities. The x (increasing i) component of the velocity u is shown as sections through the domain (a) and an arrow plot in the horizontal plane is shown in (b). Units in (a) are m/s; maximum value is 1 m/s.

Figure 4:

The induced magnetic field b_x/F_z (dimensionless) from the model based on the induction equation.

Figure 5:

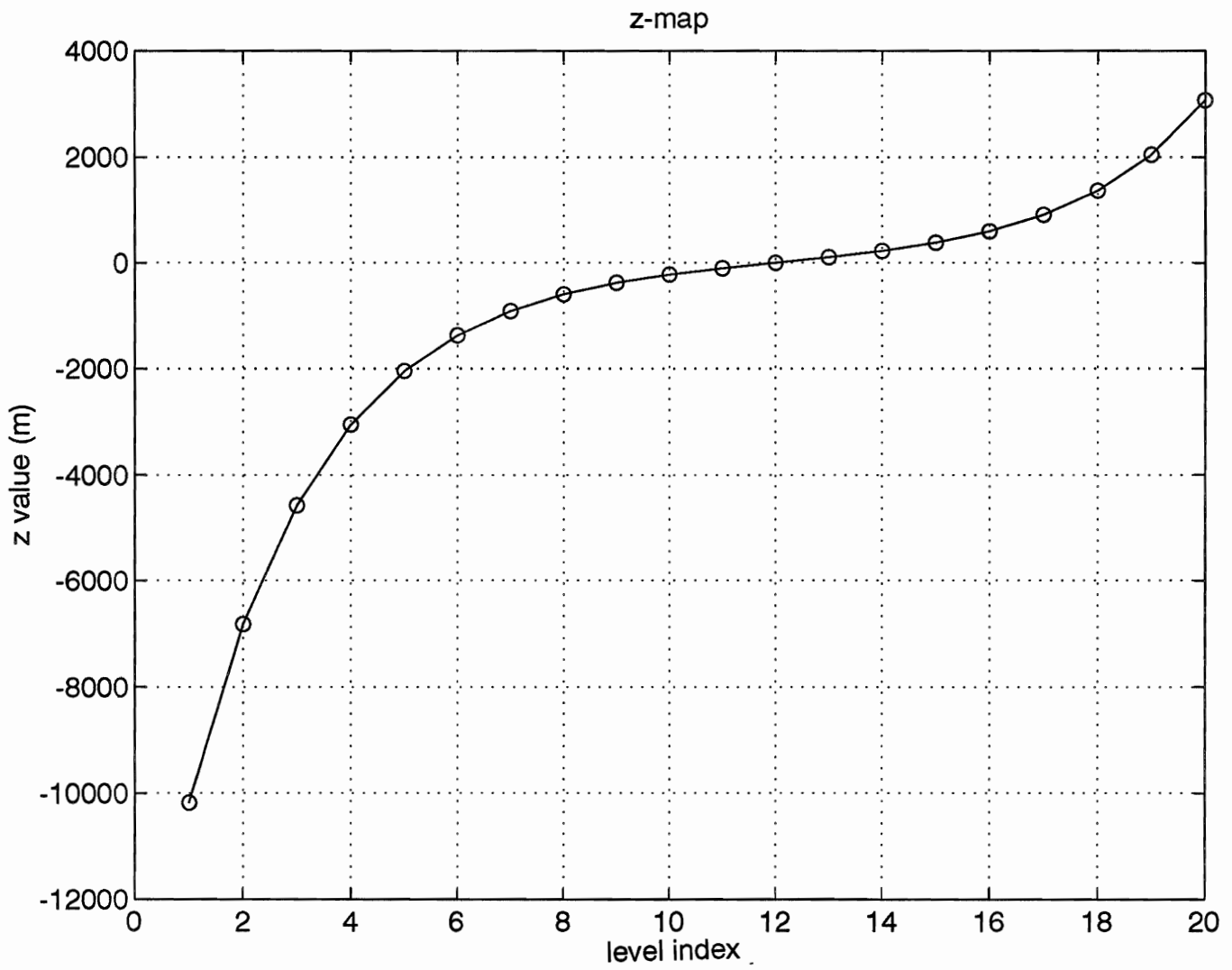
Mean of the root-squared values of b_x/F_z as a function of iteration time under the model based on the induction equation.

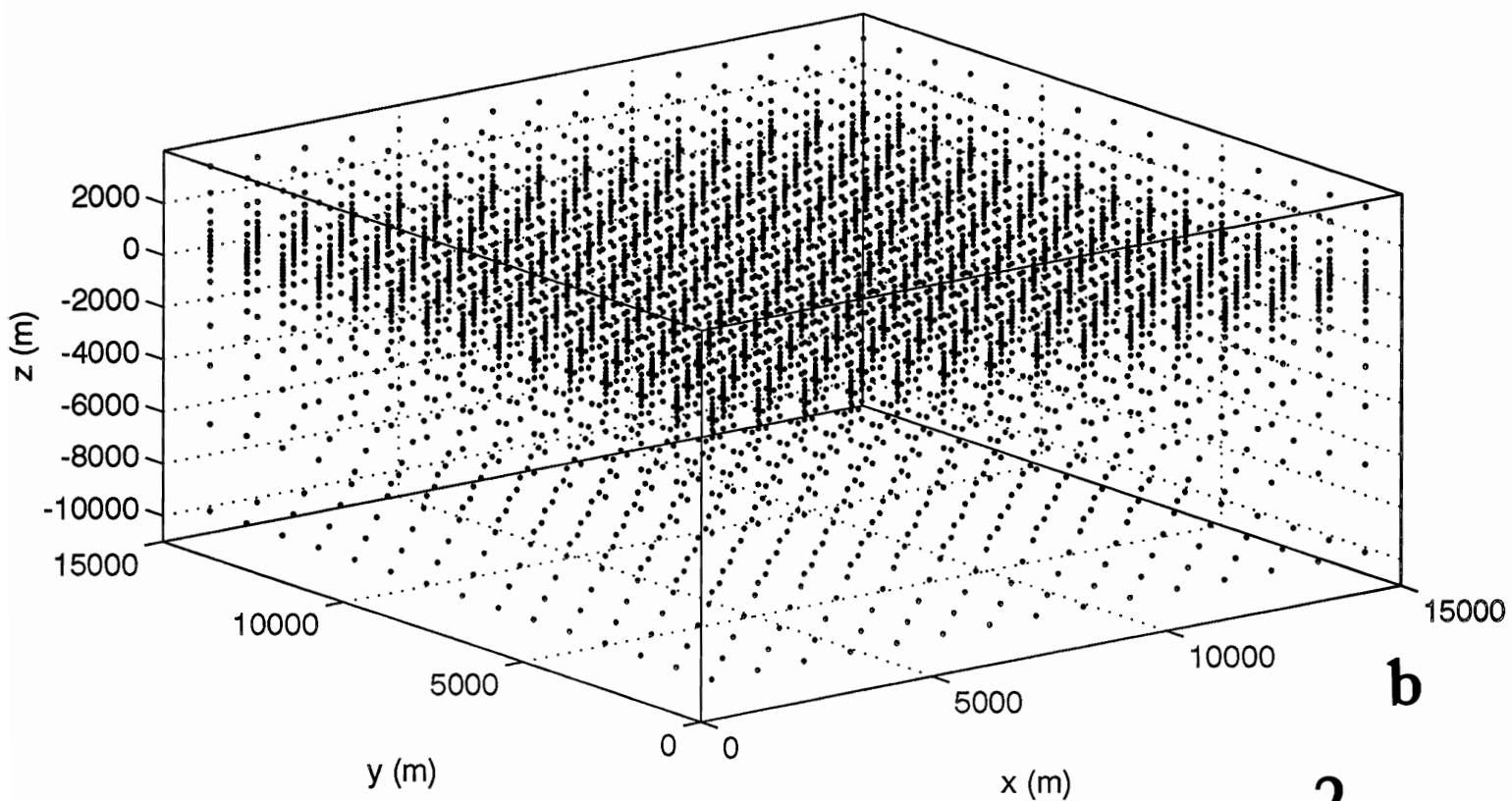
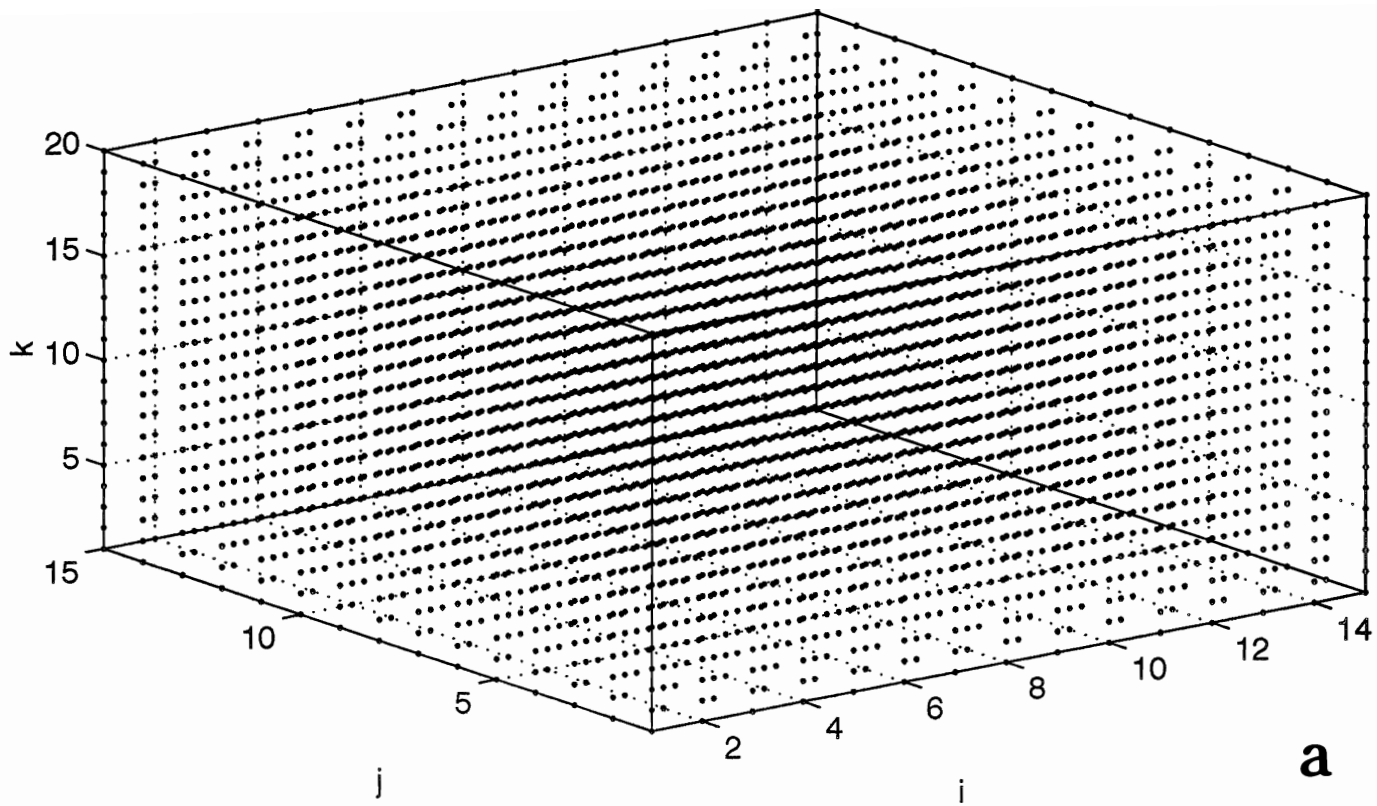
Figure 6:

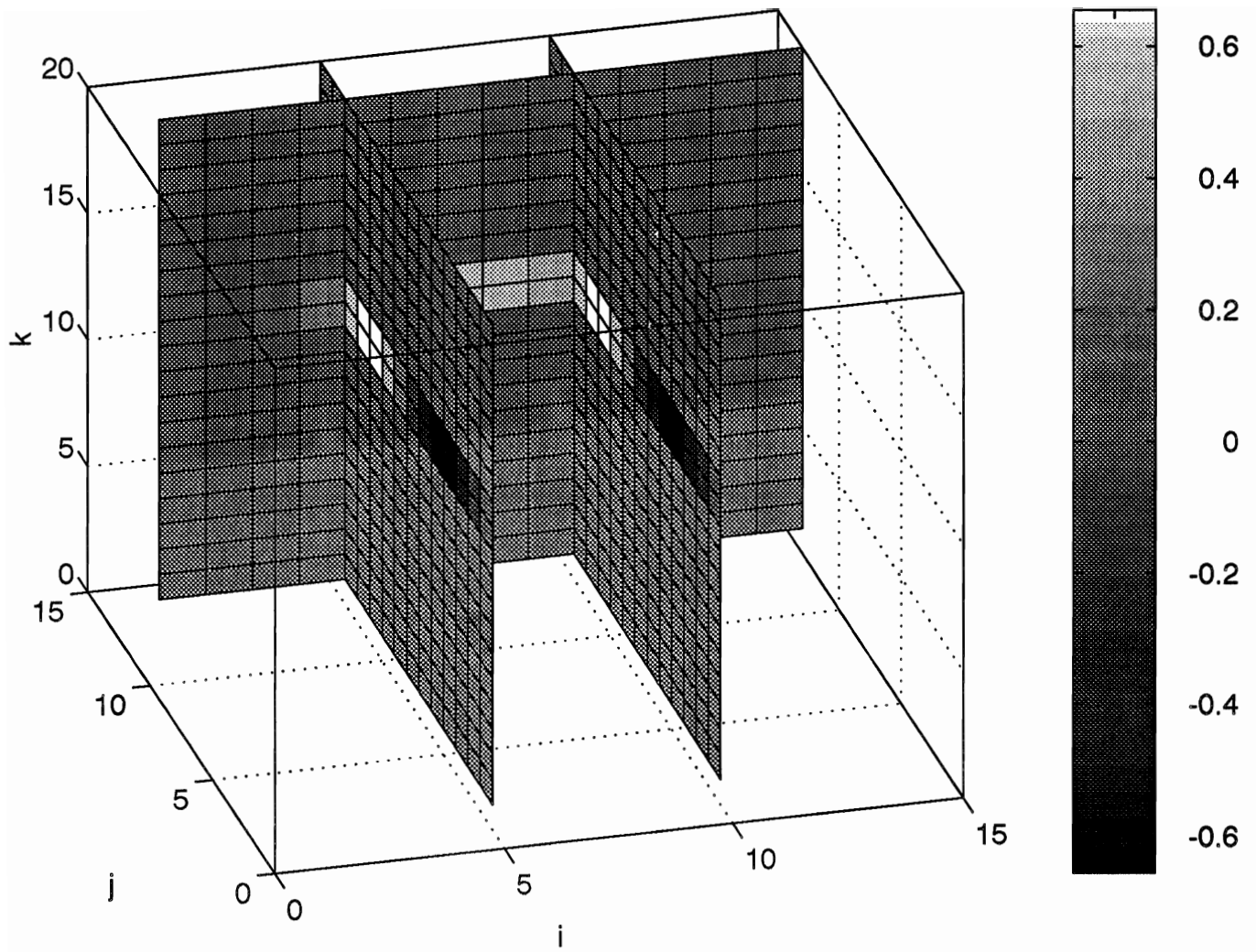
Cross-section of the electropotential ψ/F_z ($\text{V m}^{-1}\text{T}^{-1}$) (a) and induced magnetic field b_x/F_z (dimensionless) (b) from the model based on the electropotential equation.

Figure 7:

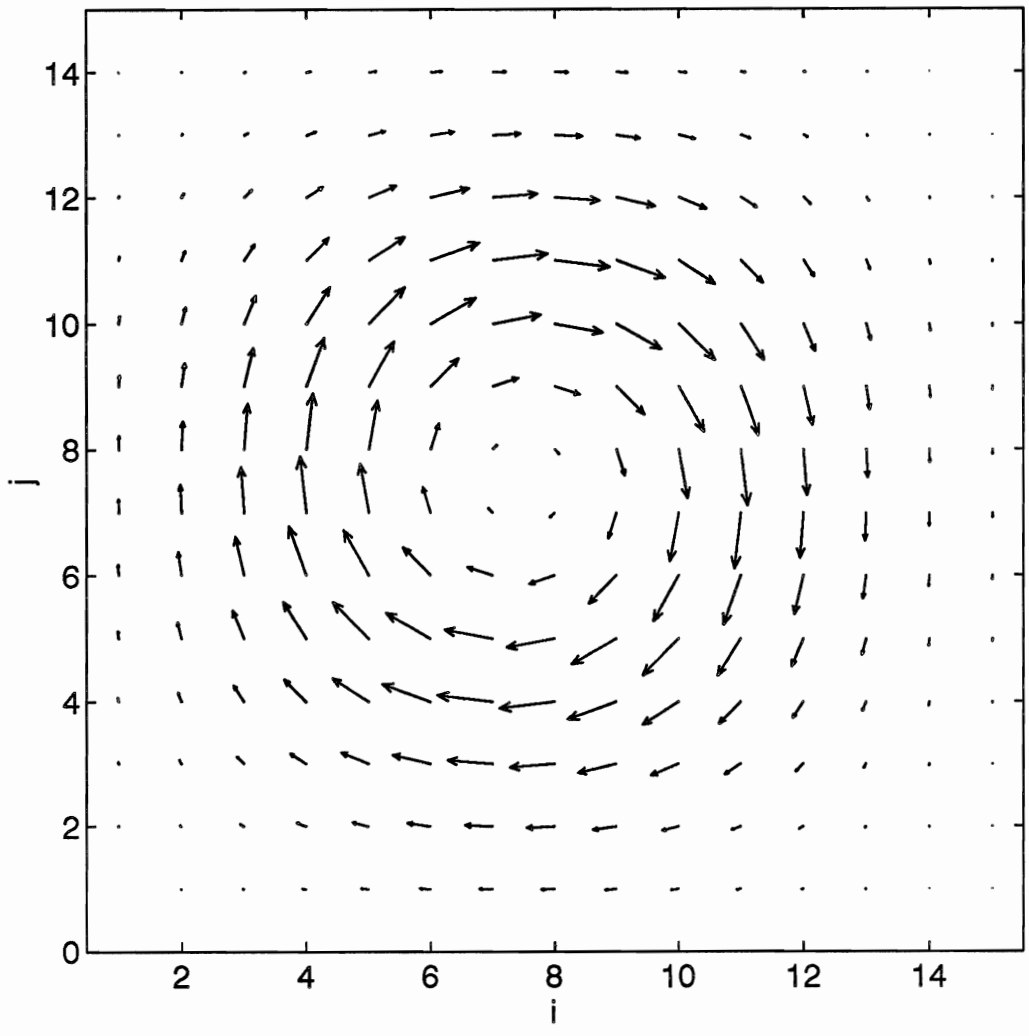
Convergence plot showing mean magnitude of the residuals (for the ψ iteration (a) and the b_x iteration (b)) from the model based on the electropotential equation.



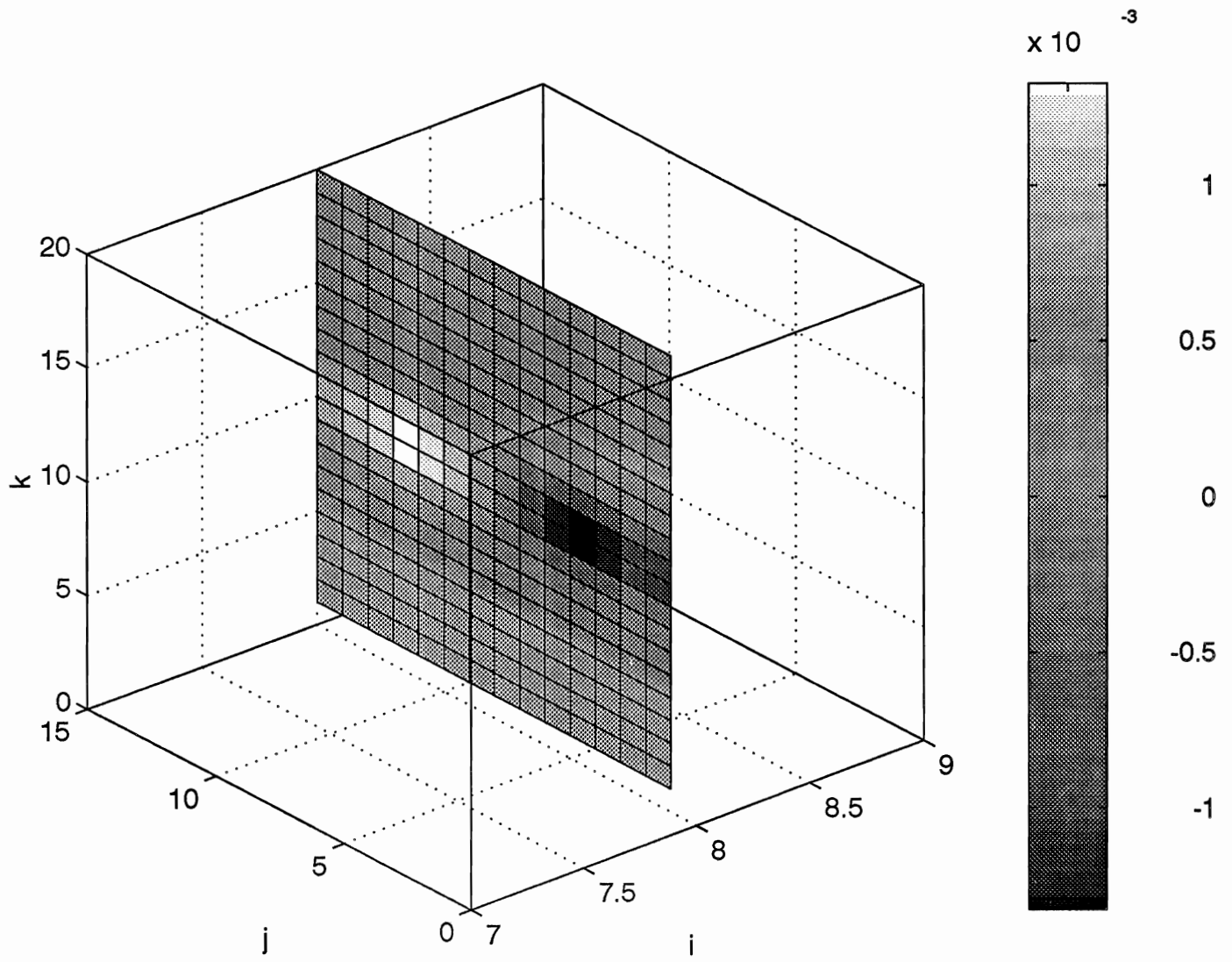


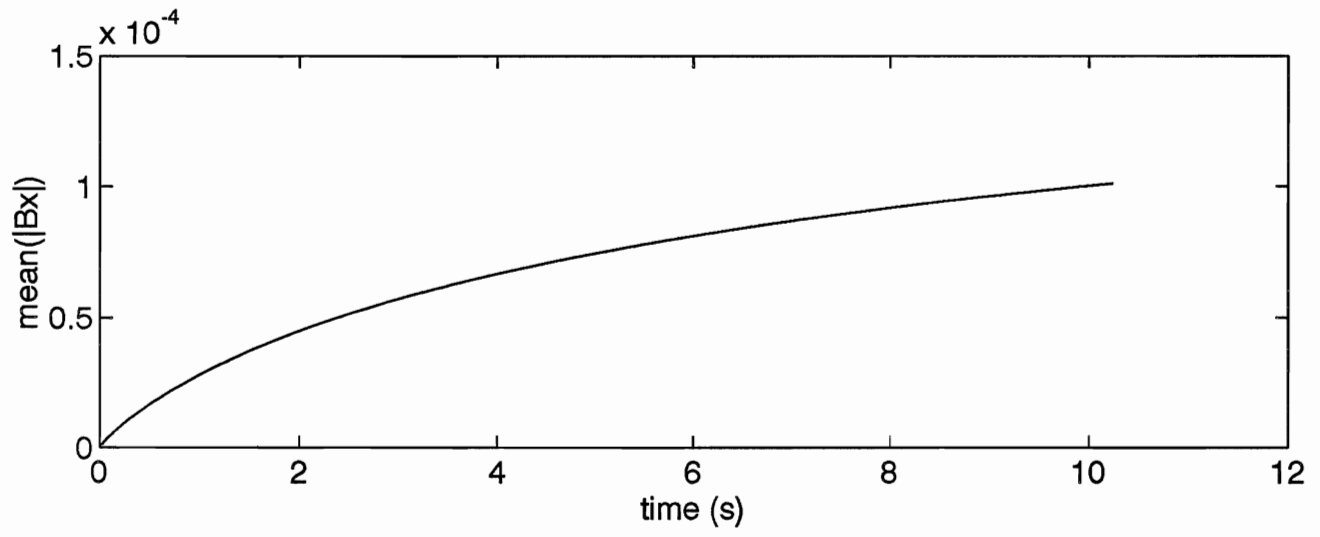


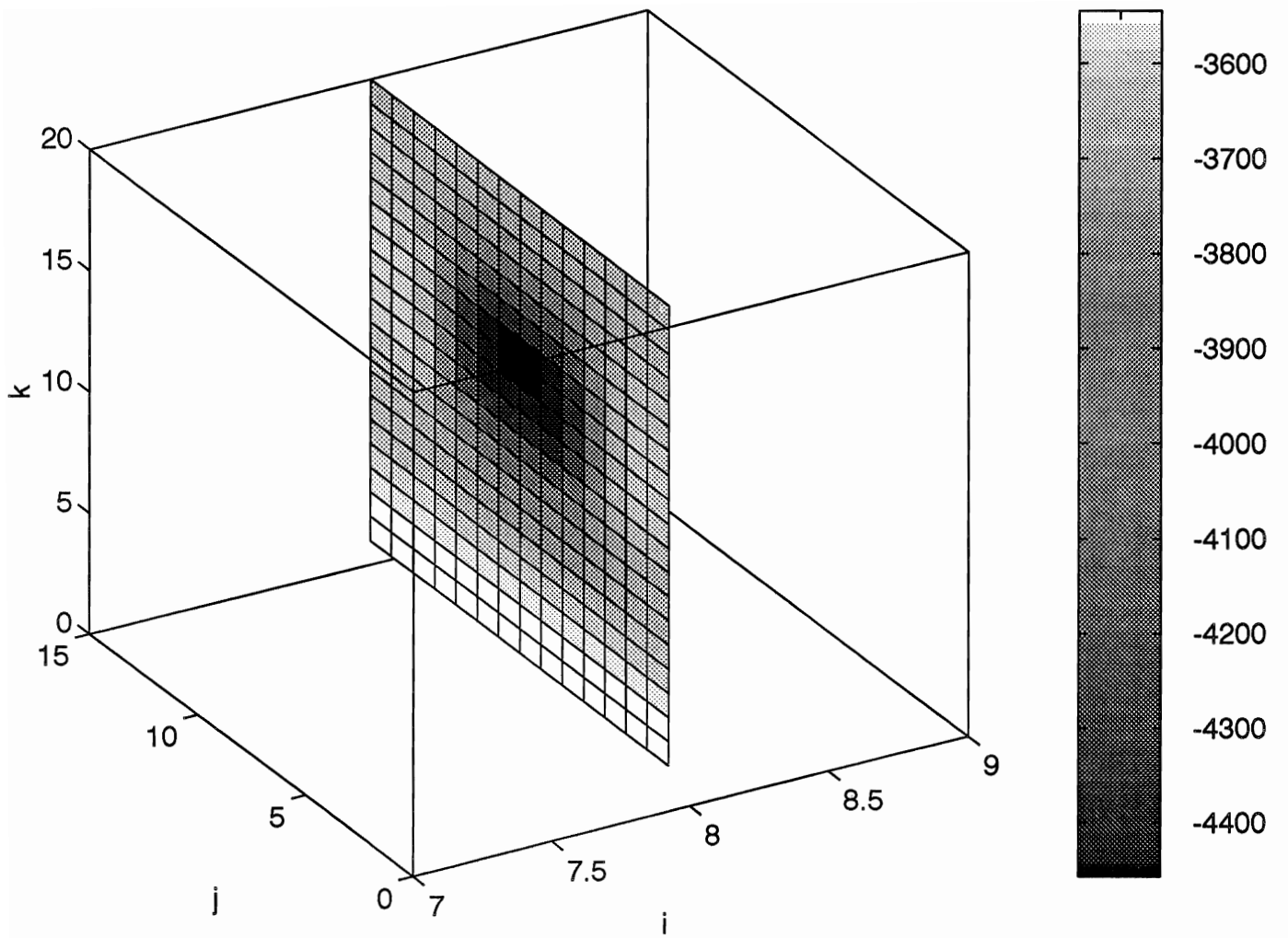
3a



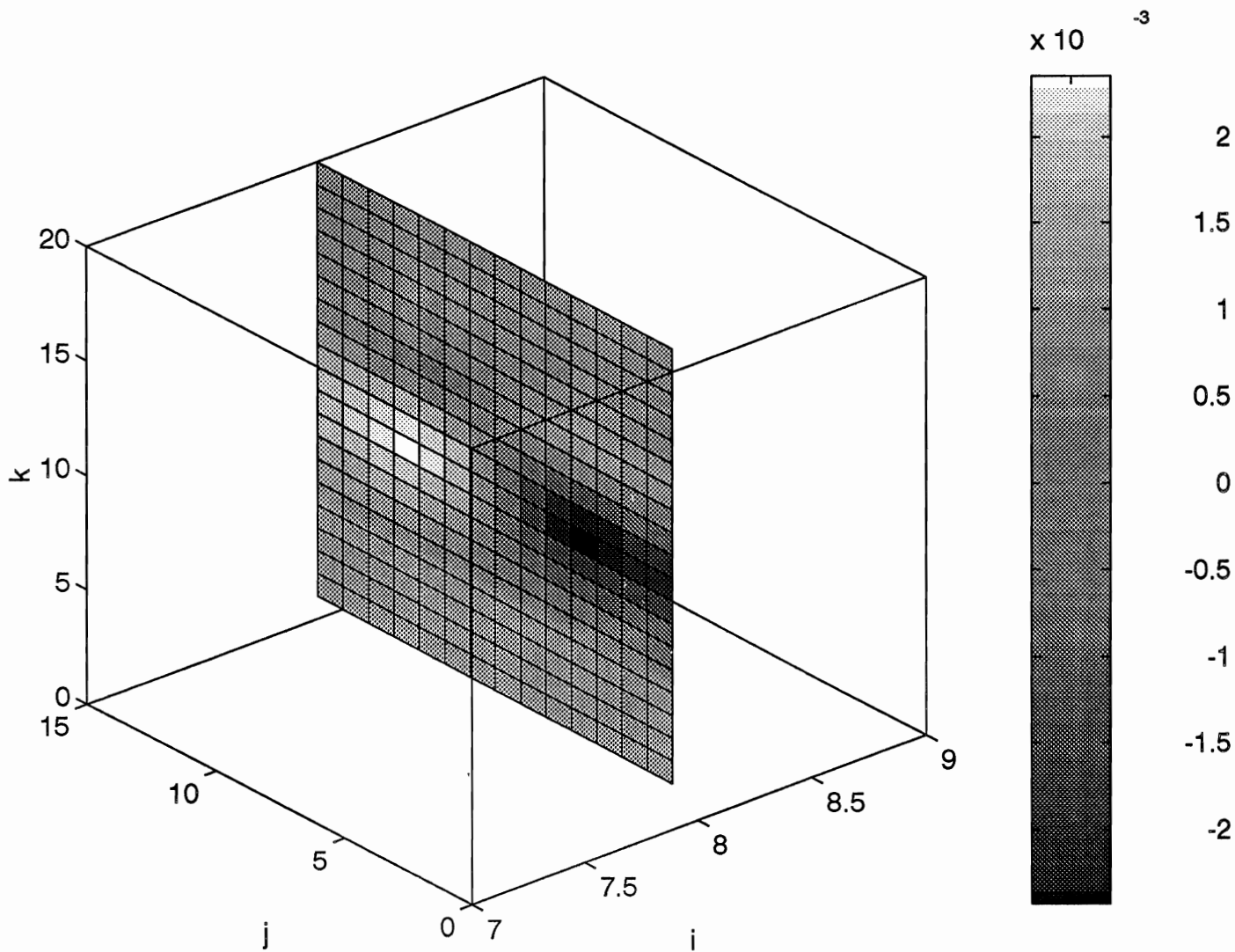
3b



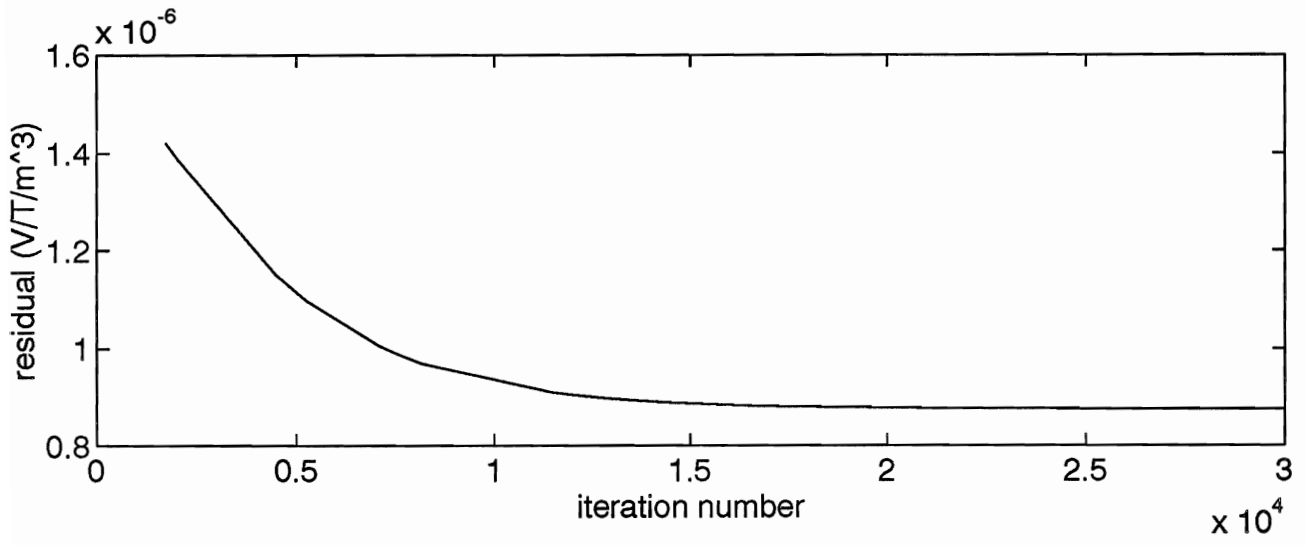




6a



6b



7a

